JOC The Journal of Organic Chemistry

Article

pubs.acs.org/joc

Planar Homotropenylium Cation: A Transition State with Reversed Aromaticity

Christopher M. Gibson,[†] Remco W. A. Havenith,[‡,⊥] Patrick W. Fowler,*[,†] and Leonardus W. Jenneskens*[,§]

[†]Department of Chemistry, University of Sheffield, Sheffield, S3 7HF, U.K.

[‡]Theoretical Chemistry, Zernike Institute for Advanced Materials and Stratingh Institute for Chemistry, Rijksuniversiteit, Groningen, Nijenborgh 4, 9747 AG Groningen, The Netherlands

[⊥]Ghent Quantum Chemistry Group, Department of Inorganic and Physical Chemistry, Ghent University, Krijgslaan 281 (S3), B-9000 Ghent, Belgium

[§]Organic Chemistry and Catalysis, Debye Institute for Nanomaterials Science, Utrecht University, Universiteitsweg 99, 3584 CG Utrecht, The Netherlands

Supporting Information

ABSTRACT: In contrast to the equilibrium structure of the homoaromatic C_s homotropenylium cation, $C_8H_9^+$ (**1**), which supports a pinched diatropic ring current, the C_{2v} transition state (**2**) for inversion of the methylene bridge of **1** is antiaromatic and supports a two-lobe paratropic π current, as detected by plotting B3LYP/6-31G** ipsocentric current maps. Participation of the bridge CH bonds is crucial for the change in global character of the current in the transition state, as shown by the quenching of its paratropicity on substitution of H by F. Orbital-based arguments allow rationalization of this transition between homoaromaticity and hyper(conjugative) antiaromaticity. More generally, the hyperconjugative ring current in a family of C_{2v} planar-constrained geometries of $(CR_2)C_{N-1}H_{N-1}^q$ homoannulenes (R = H, F) can be switched from paratropic (antiaromatic) to diatropic (aromatic) by variation of ring size, charge, and bridge substituent. An orbital-based counting rule accounts for these systematic trends.

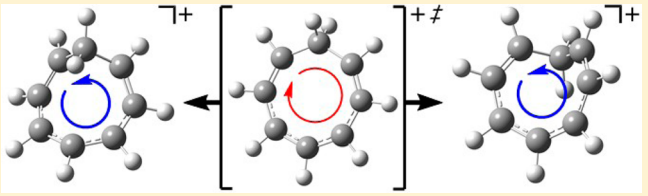

INTRODUCTION

Aromaticity appears in many guises,[1,2] each with an associated signature ring current. In the case of the archetypal 6π-homoaromatic homotropenylium cation (**1**, $C_8H_9^+$),[3−7] aromaticity of the system is corroborated by current-density maps, which show a π ring current of a peculiar character.[8] At the equilibrium geometry of **1**, a double horseshoe of conventional π current pinches down to a single σ current that flows through space under the conjugation-breaking CH_2 bridge. The experimental evidence for the horseshoe π current in **1** is based on the difference in ^{1}H chemical shifts δ_{exo} and δ_{endo} for the two types of bridge methylene site.[9] Measurement is complicated by experimental difficulties, but the estimated shift of $\Delta\delta = \delta_{endo} - \delta_{exo} = 5.8$ ppm is supported by ab initio calculation (IGLO/6-31G**//HF/6-31G*: $\Delta\delta = 5.1$ ppm[10]). Equivalent conformations of the homotropenylium cation, **1**, are formally linked by inversion of the methylene bridge, which swaps exo and endo ^{1}H nuclei (Figure 1), and can be envisaged as proceeding via an 8π C_{2v}-symmetric transition state (**2**), over a relatively high barrier of 93 kJ/mol.[11] An alternative "circumambulant" process for this transition was briefly raised but then discounted by Berson and Jenkins.[12]

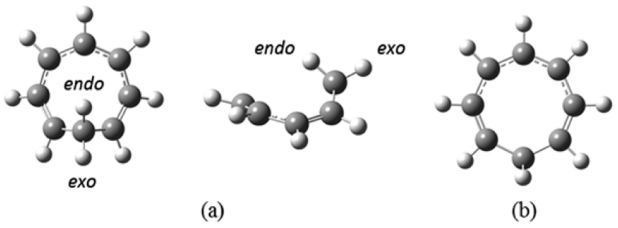

Figure 1. Optimized structures of two conformations of the homotropenylium cation $C_8H_9^+$: (a) C_s equilibrium structure, **1**, (in orthogonal views, identifying bridge exo and endo positions), and (b) C_{2v} transition state, **2**.

More recently, in a computational study of benzylic and cyclic delocalized cations,[13] the C_{2v} transition state, **2**, was found to exhibit a positive NICS(0)[14] value of +11.0 ppm at the GIAO-SCF/6-31+G*//B3LYP/6-311+G** level of theory, which would generally be taken as indicative of canonical π antiaromatic character. This value mirrors the negative NICS(0) value of −11.1 ppm computed at the same level of theory for the equilibrium structure, C_s **1**.[13] NICS values can be subject to various competing effects and are not always reliable

Received: September 22, 2014
Published: December 19, 2014

DOI: 10.1021/jo502179k
J. Org. Chem. 2015, 80, 1395−1401

indicators of current patterns; in the present case alternative explanations of this reversal of NICS values were offered,[13] but we find here that explicit calculation of ring current shows that the reversal is specifically to be associated with a transition from magnetic aromaticity of **1** to antiaromaticity of **2**. Further evidence comes from calculations by Cremer et al.,[10] who found a significant difference in magnetizability, χ, between the equilibrium (IGLO/6-31G**//HF/6-31G*: **1** $R(C_1\cdots C_7)$ = 2.285 Å, (χ/ 10^{-6} cm^3 mol^{-1}) = 86.4 calcd,[10] 72 exp[16]) and transition-state (IGLO/6-31G**//HF/6-31G*: **2**, $R(C_1\cdots C_7)$ = 2.675 Å, $\chi/10^{-6}$ cm^3 mol^{-1} = 52.9[10]) structures; in view of our results, this magnetizability difference points to ring-current antiaromaticity of the transition state.

Thus, we have the interesting situation of *reversal of aromaticity* along a reaction coordinate, corresponding to interconversion of aromatic systems via an antiaromatic transition state. We explore this process further here. We present direct theoretical evidence for the paratropic (antiaromatic) character of the C_{2v} transition state and show that this tropicity is critically dependent on the energies of the CH bonds of the CH_2 bridge, which have a π-like combination that can interact with the π system of the ring. This energy match would not be found in the CF_2 analogues of **1** and **2** (i.e., **3** and **4**), and the transition state **4** is accordingly found to be (weakly) diatropic (aromatic). Our calculations will be used to document the reversal of aromaticity between **1** and **2**, and to suggest a model for rationalizing the net tropicity of planar-constrained homoannulenes. The observation that a bridge can behave as a pseudo-π donor in these cases, with a CH_2 bridge donating two electrons,[17] will be useful here.

There are literature precedents for reversals of aromaticity in annulenes,[18−20] although the physical mechanism for these changes (Möbius twisting via cis/trans isomerization) is different from the present case where geometric motion induces a change in effective electron count.

RESULTS/DISCUSSION

Geometries of **1**−**4** were optimized at the B3LYP/6-31G** DFT level using Gaussian09.[21] In terms of the potential energy surface, if the local minimum **1** (C_s symmetry) is taken as the zero of energy, **2** is a transition state (C_{2v} symmetry, single imaginary frequency 125*i* cm^{-1}) with a relative energy of 91 kJ mol^{-1} (corrected for zero-point vibration, see Supporting Information S1). Minima and transition states were identified by Hessian calculations (see Supporting Information S1 and S2). Subsequently, current-density maps were calculated at the same level of theory using the ipsocentric CTOCD-DZ approach (CTOCD-DZ/B3LYP/6-31G**//B3LYP/6-31G**)[22] implemented in the GAMESS-UK[23] and SYMSO[24] packages, as previously[8] used for **1**. The advantages of this distributed-origin method for calculation of currents, in terms of economy and interpretability, are well documented.[25,26] A key feature for the present application to **1** and **2** is that the method gives physically nonredundant orbital contributions to current. These can be based on the use of either *canonical* (delocalized) or *localized* molecular orbitals (CMOs or LMOs) to partition the total π current density. This proves to be essential in the understanding of the maps and the interpretation of the currents in **1** and **2**.

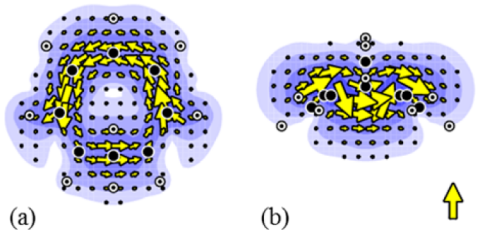

Figure 2. Diatropic ring current in the homotropenylium cation, **1**, attributable to the combined contributions of the three occupied π-like localized molecular orbitals obtained from the Pipek−Mezey procedure. (a) The horseshoe current in the ring: current density at 1.75 a_0 below the $C_1\cdots C_3\cdots C_5\cdots C_7$ reference plane[8] on the side away from the bridge (j_{max} = 0.092 au). (b) The gap-crossing current under the bridge: current density in a plane perpendicular to the $C_1\cdots C_3\cdots C_5\cdots C_7$ reference, 1 a_0 away from the $C_1\cdots C_7$ centers, on the endo (ring) side of the bridge (j_{max} = 0.101 au). Plotting conventions: arrows show the current density resolved into the plotting plane; contours show the modulus of the full current-density vector; anticlockwise circulations are diatropic and clockwise circulations paratropic. An arrow representing the "standard" benzene ring current, calculated at a plotting height of 1 a_0, is included for comparison (modulus |j| = 0.079 au at the present level of theory[22]).

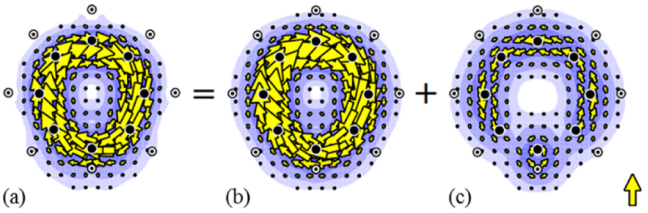

Figure 3. CMO contributions to current density of C_{2v} transition state **2**, from (a) all four occupied π-orbitals, (b) the paratropic π-HOMO, and (c) the diatropic π complement of the HOMO (i.e., map a *minus* map b). Maps are plotted at a height of 1 a_0 above the molecular plane, with plotting conventions and benzene standard arrow as in Figure 2. Orbitals of π character are defined solely by their symmetry with respect to reflection in the plane of the ring.

In the low symmetry of system, **1**, there is no formal separation of σ and π molecular orbitals, and the CMOs necessarily have mixed character. However, each carbon atom not involved in the methylene bridge has three coplanar single bonds,[8] allowing definition of an orthogonal π atomic orbital on each center[27] and construction of π-like localized molecular orbitals (LMOs) by combination. Nearest-neighbor interactions are of p_π-p_π type around the formally conjugated portion of the ring but have p_σ-p_σ character in the $C_1\cdots C_7$ bridge region. Pipek−Mezey localization[28] was used to find these combinations and their contributions to current.[29] The Pipek−Mezey LMOs for **1** here include three ring-localized π-like occupied orbitals, contributing both the horseshoe of conventional π ring current and the single stream of current crossing from carbon C_1 to C_7 under the methylene bridge, as seen in Figure 2. Note that the two CH bonds in the bridge give rise to two LMOs which contribute neither to the π current around the ring nor to the current crossing the $R(C_1\cdots C_7)$ gap in C_s **1**.[8] However, in the C_{2v} symmetry of **2**, these CH-bonding orbitals make a contribution (see below).

The transition state **2** has higher C_{2v} symmetry and hence a well-defined σ/π separation. Figure 3 shows the calculated π current maps for this system. The gap-jumping diatropic ring current of **1** has disappeared and has been replaced by a paratropic circulation that follows closely the line of carbon centers, with strength 0.096 au (as measured by j_{max}, the in-plane maximum in the current density per unit inducing

DOI: 10.1021/jo502179k
J. Org. Chem. 2015, 80, 1395−1401

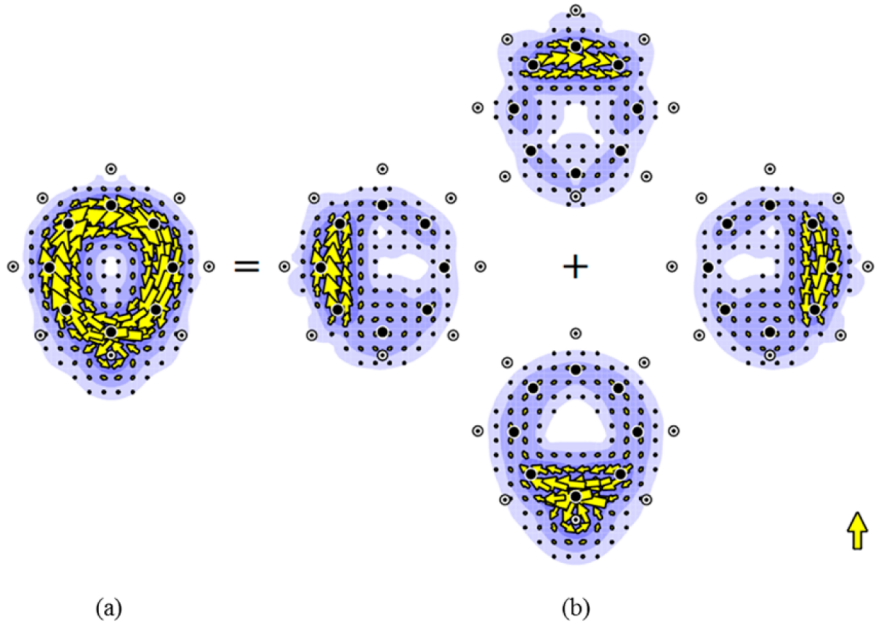

Figure 4. LMO breakdown of the π-current in the C_{2v} transition state **2**. (a) The total (five-LMO) π current map. (b) Maps corresponding to the three LMO contributions to the "horseshoe" of π ring current (top, left and right), and the current from the CH-bridge LMO contributions that complete the circulation (bottom). Plotting conventions and benzene reference arrow as in Figure 3

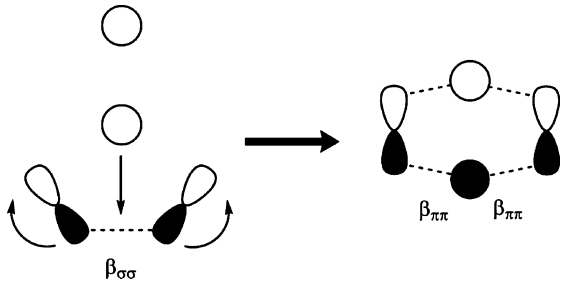

Figure 5. Pictorial model for the transformation between homoaromatic "6π" C_s **1** and hyperantiaromatic "8π" C_{2v} **2**. During the geometric change, the CH_2 bridge descends, breaking the $\beta_{\sigma\sigma}$ link of **1** and forming two $\beta_{\pi\pi}$ links, resulting in the complete "π" conjugation of **2**.

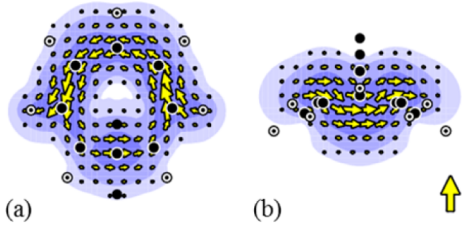

Figure 6. Diatropic ring current for the bridge-fluorinated analogue, **3**, of the homotropenylium cation. Current is attributed to the three occupied π-like orbitals obtained from the Pipek–Mezey procedure. (a) The horseshoe π current in the ring: current density 1.75 a_0 below the $C_1\cdots C_3\cdots C_5\cdots C_7$ reference plane[8] on the side away from the bridge (j_{max} = 0.058 au). (b) The gap-crossing current under the bridge: current density in a plane perpendicular to the $C_1\cdots C_3\cdots C_5\cdots C_7$ reference, 1 a_0 from the $C_1\cdots C_7$ centers on the endo (ring) side of the bridge (j_{max} = 0.046 au). Plotting conventions and benzene reference arrow as in Figure 2

external magnetic field), stronger by 20% than the standard diatropic π current in benzene.

Following the ipsocentric approach, in which total current density is partitioned into orbital contributions governed by rotational and translational symmetry selection rules,[29,30] the paratropic current is seen to arise almost entirely from the $\pi-\pi^*$ HOMO–LUMO-induced virtual excitation and is rotationally allowed as it preserves the number of angular nodes in the active orbitals. There is a close analogy with the characteristic antiaromatic current of the eight-membered cyclooctatetraene (COT) ring in planar geometries.[30] Exactly as in planar-constrained COT, the main paratropic HOMO contribution to π current in **2** (Figure 3b) is partially canceled by a weaker diatropic circulation arising from translationally allowed node-increasing excitations into the LUMO from orbitals lying immediately below the HOMO (Figure 3c). The HOMO contribution itself is dominated by the HOMO–LUMO excitation, as confirmed by spectral decomposition[31] (see Supporting Information S3). Seen in this way, **2** offers a textbook example of how the two-electron paratropic current arises in an 8π system.

The total current can be described in a basis of LMOs. This LMO description is less economical but more revealing. The occupied π molecular orbitals of C_{2v} **2** have symmetry $a_2 + 3b_1$ and correlate with the *three* occupied π orbitals of a heptatriene moiety *plus* the π-like combination of the CH bonds of the methylene bridge. As Figure 4 shows, these four orbitals taken together give rise to the closed paratropic ring current, with the heptatriene-like LMOs contributing a horseshoe of π ring current as in **1**, with continuity of the twin-loop circulation supplied by the π orbital of the CH_2 bridge.

One minor technical point alluded to earlier concerns the way that current arising from the CH-based π-like orbital is calculated. The localization procedure produces *two* spatially separated CH bonds (rather than σ and π combinations). Inclusion of *both* LMOs is therefore necessary for the maps shown in Figure 4; each of these orbitals makes a contribution to one loop of π ring current but their in-phase combination also gives rise to a small diatropic σ current concentrated in the

DOI: 10.1021/jo502179k
J. Org. Chem. 2015, 80, 1395–1401

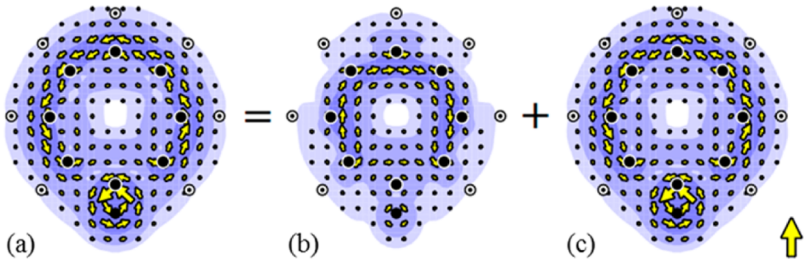

Figure 7. CMO contributions to current density of the bridge-fluorinated C_{2v} transition state, **4**, arising from (a) *all* occupied orbitals of π symmetry, (b) the paratropic π-HOMO, and (c) the diatropic HOMO complement (the difference of maps (a) and (b)). Plotting conventions and benzene reference arrow as in Figure 3

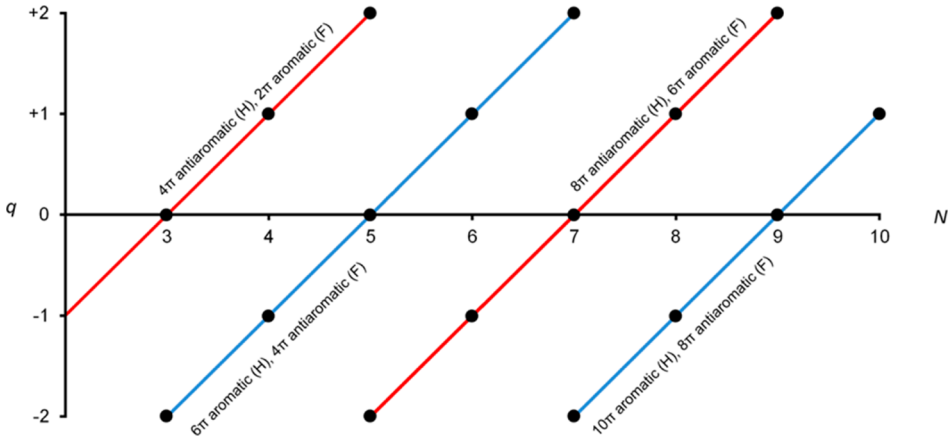

Figure 8. Classes of aromatic and antiaromatic C_{2v}-symmetric bridged annulene species $(CR_2)C_{N-1}H_{N-1}{}^q$ defined by the electron counting rule $n_\pi = N - 1 - q + \delta$, where δ pseudo-π electrons are donated by the bridge.

region exo to the bridge. This inevitable CH-based σ contamination accounts for the small differences between the canonical (four-orbital) and localized (five-orbital) π maps shown in Figures 3a and 4a, respectively. However, both are describing what is effectively a pseudo [8]annulene containing eight π-electrons.

In contrast with homoaromatic **1**, the bridge in **2** is active in transmission of the current, leading to hyperaromaticity/antiaromaticity[32] (also known as hyperconjugative aromaticity/antiaromaticity[17]). A pictorial model (Figure 5) can account qualitatively for the variation of the main features of the currents along the C_s-to-C_{2v} reaction coordinate **1**-to-**2**: the carbon centers at the "ends" of the bridge in **1** (i.e., C_1 and C_7) have planar sp^2 bonding with p_σ-p_σ overlap across the gap,[8] and the π combination of CH bonds is not sterically available in **1**. As the system moves along the inversion coordinate, p_π functions at the ends of the bridge *dis-rotate* toward parallel alignment with each other, and concomitantly the CH_2 group descends into the widening gap between carbon centers C_1 and C_7. In the limit, the cyclic "6π" system, completed by a $\beta_{\sigma\sigma}$ C−C resonance integral across the gap, becomes an "8π" system with two $\beta_{\pi\pi}$ C−H integrals crossing the gap.

An IRC-following calculation suggests that the switchover from diatropic to paratropic ring current takes place roughly halfway along the intrinsic reaction coordinate defined by the geometries of **1** and **2** (see Supporting Information S4). The crucial role of the CH bonds in providing continuity in the paratropic ring current of **2** is already evident from this localized analysis and is confirmed by comparison with the analogous system where there are CF bonds in the bridge. This fluorinated system **3** also has C_s symmetry at equilibrium ($R(C_1\cdots C_7)$ = 2.254 Å (see Supporting Information S1 and S2)) and supports a homoaromatic ring current with the "pinched" signature found in **1** (Figure 6).[8] However, the C_{2v}-symmetric transition state **4** (relative energy corrected for zero-point vibration 70 kJ mol^{-1}, with single imaginary frequency 51*i* cm^{-1}), for interconversion of minima **3**, is strikingly different from **2** in that it now displays a *weak diatropic* rather than a *strong paratropic* current. As Figure 7 shows, the total π current in **4** is dominated not by the π-HOMO orbital contribution, which is still weakly paratropic, but by the diatropic contribution from the HOMO-complement.

Comparative analysis of the frontier orbitals for **2** and **4** reveals the source of this discrepancy. The HOMO−LUMO gap is *larger* in **4** (Δ_{HL} (**2**) = 2.62 eV, Δ_{HL} (**4**) = 3.34 eV), and there is an accompanying change in *topology* of the HOMO; in **2** the HOMO−LUMO excitation is rotational in character, as both orbitals have four lobes on each face of the ring, one localized on the CH_2 fragment, whereas in **4** reduced participation of the CF_2 fragment leads to a HOMO that has three lobes on each ring face and a poorer rotational match to the LUMO (see Supporting Information S5). Both effects contribute to attenuation of the orbital paratropic current: if the energy difference is too large, continuity of the current will be disrupted; if the nodal character is unchanged, the sense of the current will not reverse. In the CF_2 analogues of **1** and **2**, the π combination of CF bonds has a lower energy, resulting in poorer interaction with the ring π orbitals, even in the optimal alignment of the planar transition state (see Supporting Information S5).

An interesting alternative interpretation of the effect of F → H substitution is proposed by Fernández et al.,[17] who suggest

DOI: 10.1021/jo502179k
J. Org. Chem. 2015, 80, 1395−1401

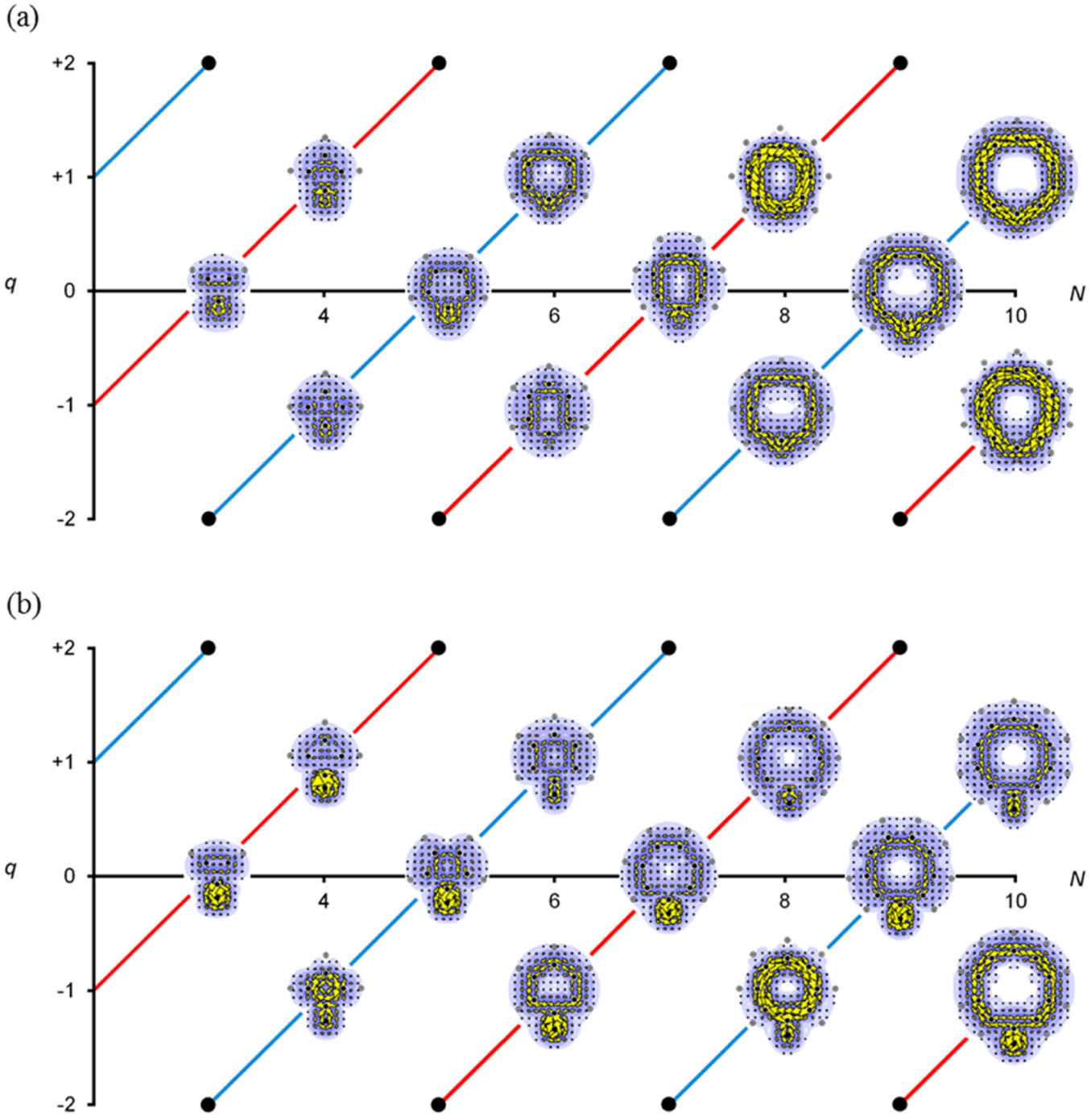

Figure 9. Current-density maps for C_{2v}-constrained bridged homoannulenes, $(CR_2)C_{N-1}H_{N-1}^{q}$, with (a) R = H, and (b) R = F. Species are arranged according to N and q as in Figure 8. Maps show total current arising from the full set of canonical π-like orbitals.

that the CR_2 unit in charge-neutral planar bridged cyclopolyenes *always* provides a pseudo-π orbital and adds two to the "π" electron count for R = H, but zero for electronegative R = F. This binary choice concentrates on electron counting rather than the subtle continuous variation of orbital energetics and topology and is based on a very restricted choice of bridge groups.

■ GENERALIZATIONS

Finally, we note that similar reasoning can be applied to give a Hückel-like model of currents in the planar-ring geometries of analogues of **2** and **4**, allowing for different ring sizes, charges, and electron counts (Figure 8). Consider a C_{2v}-symmetric structure for the species $(CR_2)C_{N-1}H_{N-1}^{q}$, derived formally by insertion of a (CR_2) bridge in a C−C bond of a (possibly charged) [*N*-1]annulene. The precise form taken by the model for ring current in this species depends on the role assigned to the bridge. In the version implied by the interpretation of Fernández et al.,[17] the bridge is assumed always to provide a pseudo-π orbital compatible in energy with the conventional sp^2 π system of the remainder of the ring. Differences between CR_2 bridges are attributed to differing numbers of electrons donated by the bridge, governed by changes in relative electronegativity of R. The (CR_2)-bridged C_{2v} structure is

DOI: 10.1021/jo502179k
J. Org. Chem. 2015, 80, 1395−1401

then a pseudo-[N]annulene. Counting gives $n_\pi = N - 1 - q + \delta$ electrons in the π system, where δ is the number of electrons donated by the (CR_2) group, and in the cases considered, n_π is always an even number. In the case of CH_2 or $C(SiMe_3)$, the bridge is taken to donate two electrons, but in the case of CF_2, none.[17] Ring currents in the species $(CR_2)C_{N-1}H_{N-1}{}^q$ can then be derived from the ipsocentric model for annulenes by consideration of the nodal structures of the HOMO and LUMO.[30]

When n_π is divisible by 4, the π HOMO and LUMO for the planar geometry are connected by a rotationally allowed transition, giving rise to a paratropic HOMO current in the ipsocentric model.[30] Conversely, when n_π is not divisible by 4, the HOMO−LUMO transition is translationally allowed and the HOMO current is diatropic. Thus, for fixed N and q, if the CH_2-bridged species is paratropic, the CF_2-bridged species is diatropic, and vice versa. Current strengths may differ, as excitations span energy gaps of different sizes.

To test this electron counting scheme, calculations were carried out on an extended series of neutral and charged systems $(CR_2)C_{N-1}H_{N-1}{}^q$ with R = H and F, N = 3 to 10, and q = −1, 0, +1, with q = 0 for odd N, and $q \neq 0$ for even N, making 24 closed-shell systems in all (see Supporting Information S6). Structures with the ring constrained to planarity were optimized at the B3LYP/6-31G** level, and ipsocentric current-density maps were computed at the CTOCD-DZ/B3LYP/6-31G** level.

According to the case, minima, transition states, or stationary points of higher order were found (see Supporting Information S7 and S8 for details). Where the planar geometry corresponded to a transition state, the imaginary frequency represented the expected conjugation-breaking mode in which the bridge moves out of the molecular plane to yield a C_s symmetric minimum (see Supporting Information S9 for details). Stationary points of higher order were typically found for the larger values of N (e.g., N = 9 and 10), with extra imaginary frequencies for distortion of the ring. However, we note that ring currents have been shown to be surprisingly robust under such conformational distortions, e.g., in the conversion of planar COT to the equilibrium tub shape,[29] where the σ/π distinction is lost as soon as the structure departs from planarity, but an identifiable π current persists for much of the pathway.

The current-density maps are collected in Figure 9. It can be seen that the new n_π rule is successful in predicting the sense of π ring current for each planar or planar-constrained system, capturing the aromatic/antiaromatic alternation with changes in either electron count or ring size, and the inversion of behavior between H and F species at the same electron count. This is effectively a generalized Hückel counting rule.

The NICS calculations of Fernández et al.[17] on the *neutral* odd cyclic polyenes are consistent with the currents calculated here, fitting neatly into the overall pattern for neutral and charged systems with different ring sizes.

In the pure "annulene" form described above, the model is an oversimplification, as it ignores differences in energy between C−C π bonds and the C−R σ bonds of the bridge. If the discrepancy in energy is too great, loss of conjugation and extinction of ring current can be expected. If desired, this feature could be accommodated by treating the CR_2 bridge as a pseudo heteroatom with full electron count of two, but with variable Hückel parameters. The general tendency would be for gaps to open up and for current to decrease, as the parameters were allowed to diverge from the values appropriate to sp^2 carbon. As the maps in Figure 9 show, current *is* generally weakened when F is substituted for H in the bridge, which is consistent with a modification of the pure annulene model. The advantage of a variable-parameter model would be that it could accommodate "mixed" situations. If the bridging group were CHF, for example, the parameters would be close to averages of CH_2 and CF_2 values, and indeed, when ab initio current maps are calculated for this mixed system, the π current is found to be very weak and paratropic (see Supporting Information S10). It is not clear how a pure electron-counting model would deal with this case.

CONCLUSION

Mapping of currents has been used to explain some initially surprising reversals of ring current in homoannulenes, giving a more detailed picture that could not be deduced from single-point calculations of properties such as NICS values, or solely by drawing MO pictures. NICS values have multiple contributions,[15] and although electron delocalization is a precondition for global current, the fact that delocalized orbitals can be constructed does not inevitably lead to ring current.[33] The interplay of orbital nodal character and energetics, however, can be used to derive a simple orbital-based interpretation of aromaticity and antiaromaticity within the homoannulene family.

ASSOCIATED CONTENT

Supporting Information

Cartesian coordinates and salient structural information for all systems, detailed analysis of structures **2** and **4**, IRC following ring current calculations for the conversion between **1** and **2**, and details of the mixed CHF-bridged case. This material is available free of charge via the Internet at http://pubs.acs.org.

AUTHOR INFORMATION

Corresponding Authors

*E-mail: p.w.fowler@sheffield.ac.uk.
*E-mail: l.w.jenneskens@uu.nl.

Notes

The authors declare no competing financial interest.

ACKNOWLEDGMENTS

R.W.A.H. thanks Prof. Dr. R. Broer (University of Groningen, The Netherlands) for fruitful discussions and acknowledges the Zernike Institute for Advanced Materials of the University of Groningen for financial support (Dieptestrategie program). C.M.G. thanks the University of Sheffield for a Ph.D. studentship.

REFERENCES

(1) Minkin, V. L.; Glukhovstev, M. N.; Simkin, Y. B. *Aromaticity and Antiaromaticity. Electronic and Structural Aspects*; Wiley: New York, 1994.
(2) Williams, R. V. *Chem. Rev.* **2001**, *101*, 1185−1204 and references cited..
(3) Von Rosenberg, J. L., Jr.; Mahler, J. E.; Pettit, R. *J. Am. Chem. Soc.* **1962**, *84*, 2842−2843.
(4) Keller, C. E.; Pettit, R. *J. Am. Chem. Soc.* **1966**, *88*, 604−606.
(5) Keller, C. E.; Pettit, R. *J. Am. Chem. Soc.* **1966**, *88*, 606−607.
(6) Childs, R. F.; Varadarajan, A.; Lock, C. J. L.; Faggiani, R.; Fyfe, C. A.; Wasylishen, R. E. *J. Am. Chem. Soc.* **1982**, *104*, 2452−2456.

DOI: 10.1021/jo502179k
J. Org. Chem. 2015, 80, 1395−1401

(7) Childs, R. F.; Faggiani, R.; Lock, C. J. L.; Mahendran, M. *J. Am. Chem. Soc.* **1986**, *108*, 3613−3617.
(8) Lillington, M.; Havenith, R. W. A.; Fowler, P. W.; Baker, J.; Jenneskens, L. W. *Phys. Chem. Chem. Phys.* **2014**, *16*, 11566−11572.
(9) Winstein, S.; Kaesz, H. D.; Kreiter, C. G.; Friedrich, E. C. *J. Am. Chem. Soc.* **1965**, *87*, 3267−3269.
(10) Cremer, D.; Reichel, F.; Kraka, E. *J. Am. Chem. Soc.* **1991**, *113*, 9459−9466.
(11) Winstein, S.; Kreiter, C. G.; Brauman, J. I. *J. Am. Chem. Soc.* **1966**, *88*, 2047−2048.
(12) Berson, J. A.; Jenkins, J. A. *J. Am. Chem. Soc.* **1972**, *94*, 8907−8908.
(13) Reindl, B.; Clark, T.; Schleyer, P. v. R. *J. Phys. Chem. A* **1998**, *102*, 8953−8963.
(14) Schleyer, P. v. R.; Maerker, C.; Dransfeld, A.; Jiao, H.; Hommes, N. J. R. v. E. *J. Am. Chem. Soc.* **1996**, *118*, 6317−6318.
(15) Steiner, E.; Fowler, P. W. *Phys. Chem. Chem. Phys.* **2004**, *6*, 261−272.
(16) Dauben, J. H. J.; Wilson, J. D.; Laity, J. L. *Nonbenzenoid Aromatics*; Snyder, J. P., Ed.; Academic Press: New York, 1967; Vol. 2, pp 167−206.
(17) Fernández, I.; Wu, J. I.; Schleyer, P. v. R. *Org. Lett.* **2013**, *15*, 2990−2993.
(18) Mauksch, M. Excursions into Chemical Topology - Topomerisations, Chiral Enantiomerisations and Möbius Aromaticity. Ph.D. Thesis, Friedrich Alexander Universität Erlangen-Nürnberg, 1999.
(19) Castro, C.; Isborn, C. M.; Karney, W. L.; Mauksch, M.; Schleyer, P. v. R. *Org. Lett.* **2002**, *4*, 3431−3434.
(20) Castro, C.; Karney, W. L. *J. Phys. Org. Chem.* **2012**, *25*, 612−619.
(21) Frisch, M. J.; Trucks, G. W.; Schlegel, H. B.; Scuseria, G. E.; Robb, M. A.; Cheeseman, J. R.; Scalmani, G.; Barone, V.; Mennucci, B.; Petersson, G. A.; Nakatsuji, H.; Caricato, M.; Li, X.; Hratchian, H. P.; Izmaylov, A. F.; Bloino, J.; Zheng, G.; Sonnenberg, J. L.; Hada, M.; Ehara, M.; Toyota, K.; Fukuda, R.; Hasegawa, J.; Ishida, M.; Nakajima, T.; Honda, Y.; Kitao, O.; Nakai, H.; Vreven, T.; Montgomery, J. A., Jr.; Peralta, J. E.; Ogliaro, F.; Bearpark, M.; Heyd, J. J.; Brothers, E.; Kudin, K. N.; Staroverov, V. N.; Kobayashi, R.; Normand, J.; Raghavachari, K.; Rendell, A.; Burant, J. C.; Iyengar, S. S.; Tomasi, J.; Cossi, M.; Rega, N.; Millam, J. M.; Klene, M.; Knox, J. E.; Cross, J. B.; Bakken, V.; Adamo, C.; Jaramillo, J.; Gomperts, R.; Stratmann, R. E.; Yazyev, O.; Austin, A. J.; Cammi, R.; Pomelli, C.; Ochterski, J. W.; Martin, R. L.; Morokuma, K.; Zakrzewski, V. G.; Voth, G. A.; Salvador, P.; Dannenberg, J. J.; Dapprich, S.; Daniels, A. D.; Farkas, Ö.; Foresman, J. B.; Ortiz, J. V.; Cioslowski, J.; Fox, D. J. *Gaussian 09, Revision D.01*; Gaussian, Inc., Wallingford, CT, 2009.
(22) Havenith, R. W. A.; Fowler, P. W. *Chem. Phys. Lett.* **2007**, *449*, 347−353.
(23) Guest, M. F.; Bush, I. J.; van Dam, H. J. J.; Sherwood, P.; Thomas, J. M. H.; van Lenthe, J. H.; Havenith, R. W. A.; Kendrick, J. *Mol. Phys.* **2005**, *103*, 719−747.
(24) Lazzeretti, P.; Zanasi, R. *SYSMO package* (University of Modena). Additional Routines by Fowler, P. W.; Steiner, E.; Havenith, R. W. A.; Soncini, A., 1980.
(25) Fowler, P. W.; Steiner, E.; Zanasi, R.; Cadioli, B. *Mol. Phys.* **1999**, *96*, 1099−1108.
(26) Steiner, E.; Fowler, P. W. *J. Phys. Chem. A* **2001**, *105*, 9553−9562.
(27) Haddon, R. *J. Am. Chem. Soc.* **1988**, *110*, 1108−1112.
(28) Pipek, J.; Mezey, P. G. *J. Chem. Phys.* **1989**, *90*, 4916−4926.
(29) Steiner, E.; Fowler, P. W.; Havenith, R. W. A. *J. Phys. Chem. A* **2002**, *106*, 7048−7056.
(30) Steiner, E.; Fowler, P. W. *Chem. Commun.* **2001**, 2220−2221.
(31) Steiner, E.; Soncini, A.; Fowler, P. W. *J. Phys. Chem. A* **2006**, *110*, 12882−12886.
(32) Lawlor, D. A.; Bean, D. E.; Fowler, P. W.; Keeffe, J. R.; Kudavalli, J. S.; O'Ferrall, R. A. M.; Rao, S. N. *J. Am. Chem. Soc.* **2011**, *133*, 19729−19742.
(33) Havenith, R. W. A.; Fowler, P. W.; Fias, S.; Bultinck, P. *Tetrahedron Lett.* **2008**, *49*, 1421−1424.

DOI: 10.1021/jo502179k
J. Org. Chem. 2015, 80, 1395−1401